

EVALUATION OF BOUNDING METHODS FOR CORRELATED FAILURE MODES

D. S. Riha*
Southwest Research Institute
San Antonio, TX 78228

R. D. Manteufel†
University of Texas at San Antonio
San Antonio, TX

Abstract

Most engineering structures contain multiple failure modes or components in which the nonperformance of any of the events can lead to system failure. In addition, the different failure modes may be correlated due to common random variables between the events. In many cases the events are assumed independent and system failure is evaluated using unions and intersections of the events. However, neglecting correlation between events may lead to grossly over predicting the probability of failure. An upper and lower bound can be determined for the probability of system failure using first- and second-order techniques. While there is some contradiction in the literature, a complete treatment of first-order bounds is made in this research. The first-order bounds are identified for events with both positive and negative correlation. In practice the second-order bounds typically use a first-order approximation to the limit-state for each event and the intersection of the two events is estimated by the correlation between the events. For nonlinear limit-states, the bounds may not actually include the true solution based on the error of the event probabilities of failure or the predicted intersection of the events. Several numerical examples are used to evaluate the accuracy and effectiveness of the bounds.

Introduction and Background

Physics based modeling is now routinely used to predict the behavior and response of complex systems. Computational simulation is being increasingly used as performance requirements for engineering structures increase and as a means of reducing testing. These high fidelity models used to accurately predict the performance of complex systems may require many hours of computation time. Many of the systems being designed or evaluated have multiple failure modes or components in which the nonperformance of any of the events can lead to system failure. The failure modes are generally correlated because of common variables between the events. For a system where the failure modes are modeled as a series system, neglecting these correlations can lead to grossly over predicting the probability of system failure. One approach to computing the probability of system failure is Monte Carlo simulation. However, this approach becomes prohibitive when each failure mode requires a numerical solution such as finite element analysis.

The limitations of Monte Carlo simulation led researchers to develop approximate methods to compute the system probability of failure. One approach is to place bounds on the solution. First-order bounds were applied by Cornell¹ but have been shown to be quite wide for many practical problems. Kounias²

* Senior Research Engineer, Member AIAA

† Assistant Professor, Member AIAA

Copyright © 2001 by Southwest Research Institute.
Published by the American Institute of Aeronautics
and Astronautics, Inc. with permission.

formulated the second order-bounds for system probability of failure. These bounds proved difficult to evaluate since they also required the probability of intersection between each pair of events. Ditlevsen³ proposed a weakened version of these bounds for Gaussian variates. The approach bases the joint probability of two events on a first-order approximation of the failure space. This method is simpler to evaluate but may be inaccurate for nonlinear functions. Improvements to this first-order approximation have been proposed by Madsen et al.⁴ and Cuse⁵ that may give a better estimate of the joint probability for nonlinear functions. Cruse et al.⁶ proposed a method to numerically integrate the joint failure region based on the first-order approximations of the performance functions. This approach yields the joint probability of failure instead of bounds used by Ditlevsen.³ There are several recent text books that include the subject of system reliability by Ang and Tang⁷, Cruse⁵, Ditlevsen and Madsen⁸, Madsen et al.⁴, Rao⁹, and Throft-Christensen and Murotsu.¹⁰ However, these works include some contradiction in explanation of the first-order bounds.

Event Probability Calculation

The first step in computing system reliability is to determine the event probabilities of failure. Failure event probabilities can be determined by testing or by combining probabilistic algorithms with physics based models. The physics based models can be analytical relationships or complex numerical analysis packages such as finite element or heat transfer codes that are used to model the performance of the component or failure mode. Numerous methods for computing event probabilities of failure using physics based models are available including traditional Monte Carlo simulation, first order reliability method (FORM), second order reliability method (SORM), and the family of advanced mean value methods.¹¹

A common approach to system reliability is to compute the event probabilities using FORM. First, a limit-state is defined such that it separates the design or sample space into safe and failed regions ($g=0$). The joint probability density function (JPDF) is then integrated over the failure region to determine the probability of failure. FORM transforms the limit-state into the standard normal space to simplify the probability integration. The method uses an optimization technique to locate the minimum distance to the limit-state function. This minimum distance is the point on the limit state with the greatest joint density and is referred to as the most probable point (MPP). FORM approximates the limit-state with a linear hyper plane in the transformed space. If the true limit-state is

nonlinear, then there will be some error in the approximation to the probability of failure. These concepts are shown in Figure 1.

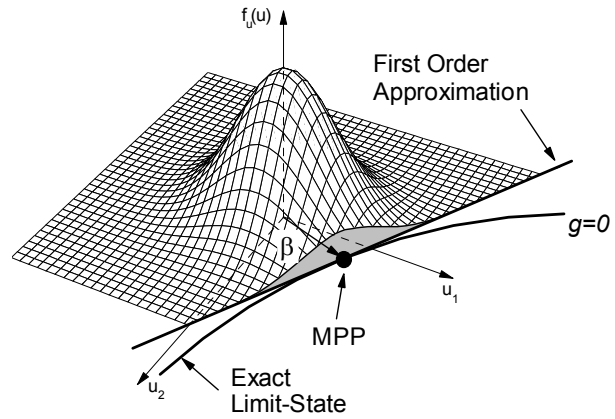


Figure 1 Joint Probability Density Function in the Transformed Space for Two Random Variables

System Reliability

Most engineering structures contain multiple failure modes or components in which the nonperformance of any of the events can lead to system failure. In addition, the different failure modes may be correlated due to common random variables between the events. When using approaches such as FORM to compute the event probabilities of failure, the degree of correlation is estimated by taking the dot product of the direction cosines to the MPP of each failure mode. This correlation measure will be increasingly inaccurate as the limit-state deviates from a linear form.

In complex multi-component systems, the different failure modes or ways the system can fail requires a systematic method to identify all failure modes and their consequences. The fault tree provides a means of identifying the failure modes and consequences. The fault tree decomposes the main failure event (system failure) into unions and intersections of events or combinations of events. In general, multiple modes of failure can be depicted as shown in Figure 2.

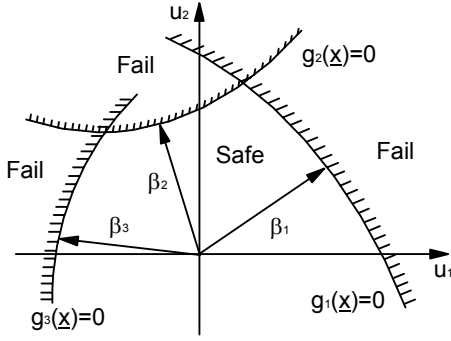


Figure 2 Limit-States and Fault Tree for Multiple Failure Modes for Two Random Variables

The probability of failure for a series system is the sum of the probability for each event minus the probability associated with the intersections of the events. The probability of failure for the events is fairly straightforward to obtain either by testing or numerical simulation. The intersection probabilities are more difficult to determine and approximations are commonly used. The intersection probability is directly related to the amount of correlation between the events. As an example, the equation for the three event union system shown in Figure 2 is

$$\begin{aligned}
 p_f = & P(E_1) + P(E_2) + P(E_3) \\
 & - P(E_1 \cap E_2) - P(E_2 \cap E_3) \\
 & - P(E_1 \cap E_3) - P(E_1 \cap E_2 \cap E_3).
 \end{aligned} \quad (1)$$

To compute the probability of failure requires the evaluation of the event probabilities along with the intersections of the events. The joint probability density function is integrated over the failure regions using the following equation

$$p_f = \int \cdots \int_{E_1 \cup \cdots \cup E_k} f_{X_1, X_2, \dots, X_n}(x_1, x_2, \dots, x_n) dx_1 dx_2 \dots dx_n \quad (2)$$

The failure regions are shown conceptually in Figure 2. Analytical evaluation of this integral is seldom possible and other approaches are commonly used.

Bounding Methods

Bounding methods attempt to determine an upper and lower value of the probability associated with the intersection of events. For correlated parallel or series system, the probability of system failure requires information about the intersection of the events. For first-order bounds, the solution can be bounded by assuming full negative or positive correlation between the events. Second-order or bi-modal bounds require accurate information about the intersection of the events and can be difficult to obtain. In practice the second-order bounds typically use a first-order approximation to the limit-state (such as a FORM solution). The intersection of the two events is estimated by the correlation between the events.

First-Order Bounds

Tighter first-order bounds can be computed if information about the correlation between the events is known. Correlation is defined as ρ and can have values between -1 and $+1$. The following sections develop the bounds for positively and negatively correlated events.

Positively Correlated Events. For positively correlated events ($0 \leq \rho \leq 1$) the bounds for the intersection probability can be determined for two events by using Figure 3. Figure 3(a) shows the intersection for independent events in the reduced variable space. The intersection probability is $P(A) \cdot P(B)$ which corresponds to the lower bound. The upper bound corresponds to full positive correlation between events as shown in Figure 3(c) and is the minimum of $P(A)$ and $P(B)$. Therefore the bounds on the intersection probability are given by

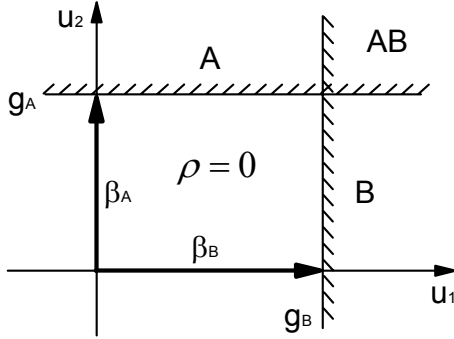
$$P(A) \cdot P(B) \leq A \cap B \leq \min[P(A), P(B)]. \quad (3)$$

Again, using Figure 3, the union probability can be bound below by the fully positive correlation assumption and above by the independent event assumption:

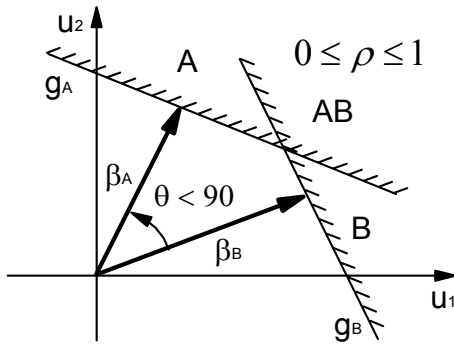
$$\begin{aligned} \max[P(A), P(B)] &\leq A \cup B \\ &\leq P(A) + P(B) - P(A) \cdot P(B) \end{aligned} \quad (4)$$

For multiple failure modes, the general form of the first-order bounds for series systems is

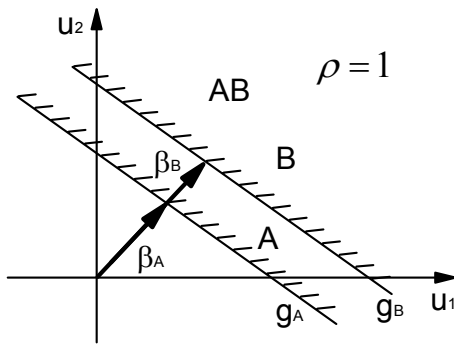
$$\max p_{f_i} \leq p_f \leq 1 - \prod_{i=1}^k (1 - p_{f_i}). \quad (5)$$



(a)



(b)



(c)

Figure 3 Limit-State Scenarios for Positively Correlated First-Order Bounds

Negatively Correlated Events. For negatively correlated events ($-1 \leq \rho \leq 0$) the bounds for the intersection probability can be determined for two events by using Figure 4. As seen in Figure 4 (a), the intersection for perfect negative correlation is zero. This is the lower bound for the intersection. The upper bound on the intersection is graphically shown by Figure 4 (c) and is the independent event case. Therefore the bounds on the intersection probability for negatively correlated events are given by

$$0 \leq A \cap B \leq P(A) \cdot P(B). \quad (6)$$

The bounds for the union of two events can be determined in a similar fashion using Figure 4. The intersection will be bounded below by the fully independent situation (c) and above by the full negative correlation case (a):

$$P(A) + P(B) - P(A) \cdot P(B) \leq A \cup B \leq P(A) + P(B). \quad (7)$$

This development can be extended to any number of events and in terms of event probabilities of failure the bounds for a series system are

$$\sum_{i=1}^k p_{f_i} - \prod_{i=1}^k p_{f_i} \leq p_f \leq \sum_{i=1}^k p_{f_i}. \quad (8)$$

Unknown Correlation. In the event that there is no knowledge of the correlation between two events, then the bound must take into account the full range of possibilities from the fully negative to fully positive correlation cases. For unknown correlation, the intersection of two events are bounded below by the full negative correlation and above by full positive correlation:

$$0 \leq A \cap B \leq \min[P(A), P(B)]. \quad (9)$$

The bounds on the union probability can be determined from Figure 3 and Figure 4. The lower bound is given when $\rho = 1$ and the upper bound is given when $\rho = -1$,

$$\max[P(A), P(B)] \leq A \cup B \leq P(A) + P(B). \quad (10)$$

This development can be extended to the general case of multiple events for a series system yielding

$$\max[p_{f_i}] \leq p_f \leq \sum_{i=1}^k p_{f_i}. \quad (11)$$

The separation of the bounds given by Equations 5, 8, and 11 will depend on the number of failure modes and on the relative magnitudes of the event probabilities of failure. If the probability of failure for a single event is large while the other events have a small probability of failure, then the probability of system failure will be

dominated by this event. In this case, the bounds will be narrow and the probability of system failure may be represented by this one event. However, for a larger number of failure modes with comparable event probability of failures, the bounds may be too wide to be of practical use.

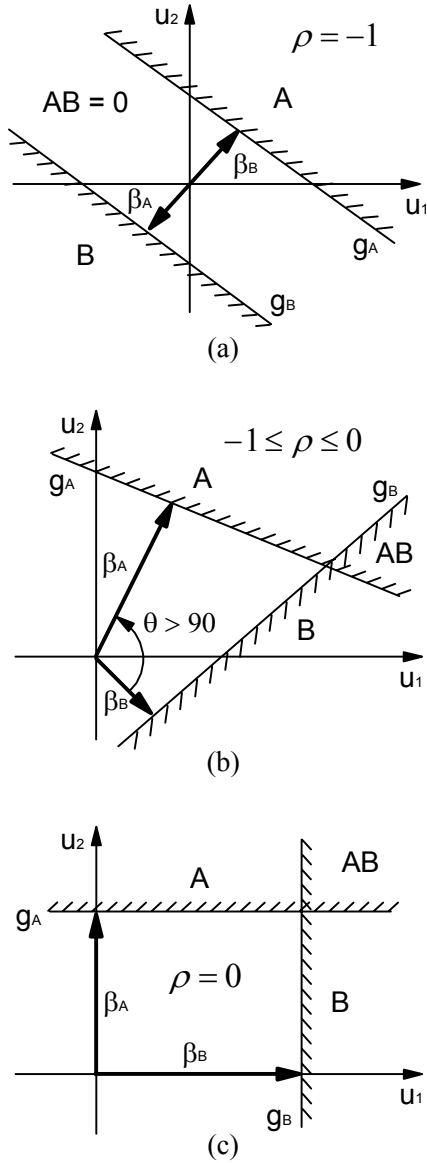


Figure 4 Limit-State Scenarios for Negatively Correlated First-Order Bounds

Second-Order Bounds

The first-order bounds can be improved by taking into account the correlation between pairs of events and bounding the intersection of two events. The resulting bounds require knowledge of the probabilities of joint

events and thus are called second-order or bi-modal bounds. The second-order bounds for k potential failure modes^{2,12} are given by

$$p_{f_i} + \max \left[\sum_{i=2}^k \left\{ p_{f_i} - \sum_{j=1}^{i-1} P(E_i E_j) \right\}; 0 \right] \leq \quad (12)$$

$$p_f \leq \sum_{i=1}^k p_{f_i} - \sum_{i=2}^k \max P(E_i E_j)$$

where p_{f_i} are the event probability of failure and $P(E_i E_j)$ are the joint event probabilities. For general problems, the joint event probabilities given in Equation 12 are difficult to calculate. In addition, the second-order bounds defined by Equation 12 will depend on the ordering of the events. The sharpest bounds can be determined by looking at the different orderings. Ang and Tang⁷ proposed examining several random orderings for large systems. Xiao and Mahadevan¹³ have shown that the upper bound reduces to the probability of intersection of the least likely failure events for practical problems.

Ditlevsen³ proposed a weakened version of the above second-order bounds for Gaussian variates. The method uses linear approximations to the limit-states and provides bounds on the intersection probability. The approximations for $P(E_i E_j)$ are used in Equation 12. The bounds are different for events with positive and negative correlation and are developed below.

Positively Correlated Events. For positively correlated events the bounds on the intersection can be determined for two linear limit-states in the reduced variable space using Figure 5(a). The approach is to construct a hyperplane perpendicular to each limit-state that passes through the intersection of the limit-states. This allows the computation of the probability volumes associated with A and B in the figure using the independent event assumption. The two distances to the perpendicular hyperplanes are developed below.

Using Figure 5, the intersection probability, $P(E_i \cap E_j)$, is bounded as

$$\max[P(A), P(B)] \leq P(E_i \cap E_j) \leq P(A) + P(B) \quad (13)$$

The probabilities of the joint events, $P(E_i \cap E_j)$, in Equation 12 are then approximated using the appropriate sides of 13. The bounds for a two event series system using Equation 12 are

$$\sum_{i=1}^k p_{f_i} - [P(A) + P(B)] \leq p_f \leq \sum_{i=1}^k p_{f_i} - \max[P(A), P(B)]. \quad (14)$$

Negatively Correlated Events. The same treatment for bounding the intersection for linear limit-states that are negatively correlated is presented using Figure 5(b). Again the perpendicular hyperplane is defined for each limit-state and the probabilities associated with A and B in the figure are determined. The lower bound for two negatively correlated events is trivially zero ($\rho=0$) and the upper bound is inferred from the figure to be the minimum of the probabilities associated with A and B. Therefore the bounds on the intersection are

$$0 \leq P(E_i E_j) \leq \min[P(A), P(B)]. \quad (15)$$

For two negatively correlated events, the bounds on the intersection using Equation 12 are

$$\sum_{i=1}^k p_{f_i} - \min[P(A), P(B)] \leq p_f \leq \sum_{i=1}^k p_{f_i}. \quad (16)$$

This method for intersection probability estimation becomes increasingly inaccurate as the limit-states become more nonlinear. Figure 6 shows an example of two nonlinear limit-states along with the linear approximations for two random variables. In the example shown, the first-order intersection may provide a large error in the intersection calculation. One approach for a better estimation would be to use an optimization procedure to locate the true intersection between the limit-states. Once this point is found the, linear approximations to the limit-states are determined at the true intersection and the computations for A and B are performed as before.⁴ The FORM solution may provide inaccurate probabilities for the event calculations of nonlinear limit-states. The true probability of system failure may not lie within the second-order bounds of Equation 12. The error in the bounds for nonlinear limit-states can be both from the event probabilities determined using FORM and the bound of the intersection using the linear limit-state assumption.

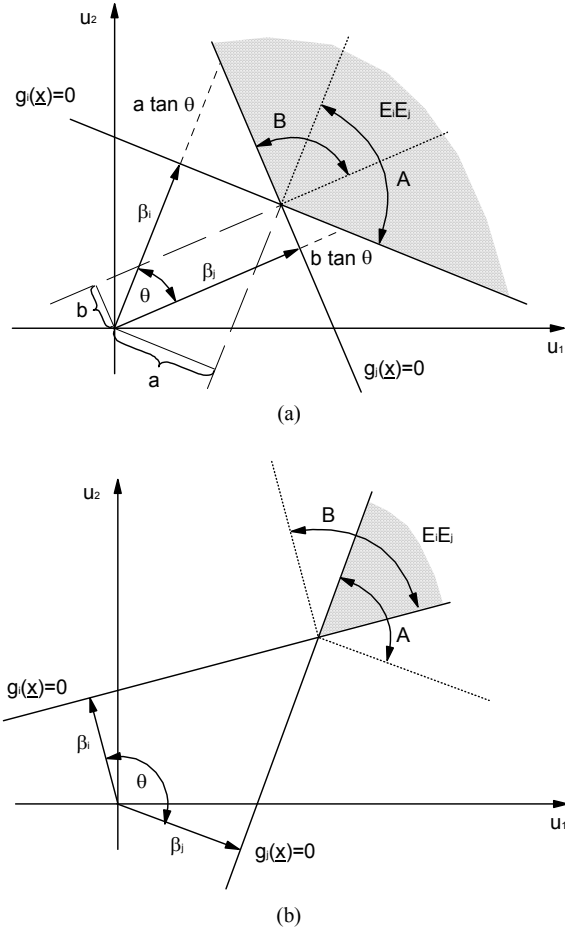


Figure 5 Tangent Planes for (a) Positively and (b) Negatively Correlated Failure Events

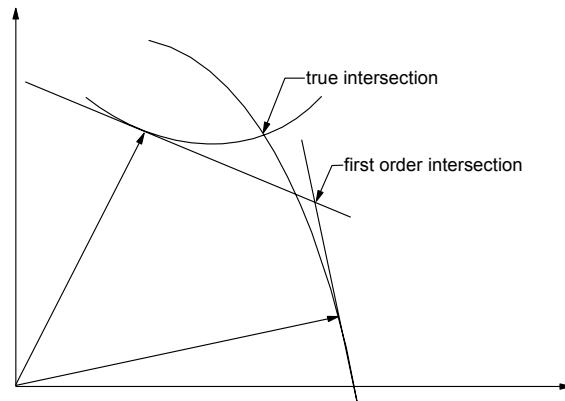


Figure 6 Example of Nonlinear Limit-States

Example Problems

A simple structural system was devised to evaluate first- and second-order bounding methods. The system consists of two failure modes of a cantilever beam. The failure modes are defined as exceeding a displacement

limit and exceeding the yield strength. Two cases are examined with different combinations of random variables. The first problem uses two normal random variables and two failure events so that the limit-states and failure regions can be shown graphically. The next problem uses all relevant random variables for the problem and assumes they are all normally distributed.

The NESSUS probabilistic analysis software was used to compute the event probabilities of failure using FORM and the system probability of failure using Monte Carlo simulation. NESSUS was originally developed under a NASA sponsored program led by Southwest Research Institute.^{14,15}



Figure 7 Cantilever Beam Problem Description

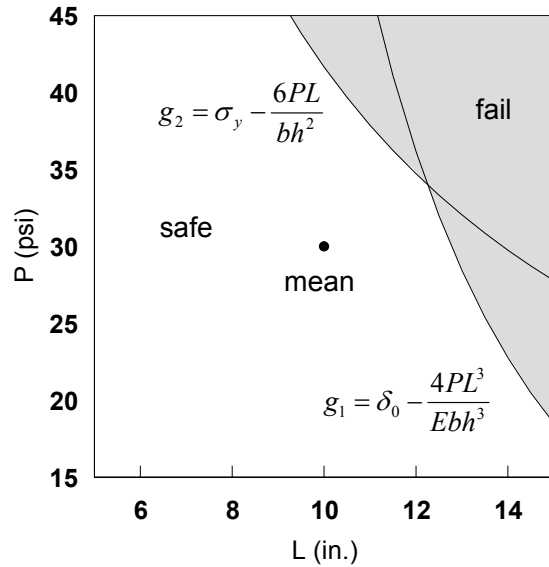


Figure 8 Limit-States for Two Random Variable Case

Two Random Variable Case

The first problem is a two-failure mode system with two normal random variables. The system is a cantilever beam and can fail by exceeding a designed displacement limit or by exceeding the yield strength. For this first problem, only two random variables are modeled so the problem can be studied graphically and solved using numerical integration. The solution using numerical integration provides a benchmark to evaluate the accuracy of the bounds. Figure 7 shows the cantilever beam and parameters. Figure 8 shows the limit-states for the two failure modes along with the equations of the limit-states. Table 1 lists the random variable statistics for this example.

Numerical integration and Monte Carlo simulation were used to compute the baseline probability of system failure and are listed in Table 2. An approach that is commonly used is to assume that the events are independent (right side of Equation 10). The independent event assumption is also listed in Table 2 and over predicts the probability of system failure by 43% but is a conservative estimate.

Table 1 Random Variables for the Two Random Variable Case

Random Variable	Description	Mean	Standard Deviation	Distribution
P	Point Load	30.0 (lb.)	3.0 (lb.)	NORMAL
L	Beam Length	10.0 (in.)	1.0 (in.)	NORMAL
E	Elastic Modulus	10,000,000.0 (ksi)	0	-
B	Beam Base	1.0 (in.)	0	-
H	Beam Height	1.0 (in.)	0	-
δ_0	Displacement Limit	0.06 (in.)	0	-
σ_y	Yield Strength	5000.0 (psi)	0	-

The FORM results for each failure event are listed in Table 6. The MPP information is also included and the correlation between these events is estimated to be $\rho = 0.91$. Therefore, the first and second-order bounds for positively correlated events are computed using Equations 8 and 14 respectively. The bounds are shown in Table 3.

The first-order bounds correctly enclose the true solution but are quite wide. The second-order bounds provide a much better estimate of the system probability of failure. Because of the high degree of positive correlation for this problem, the lower bounds for both approaches are closer to the true probability of system failure.

Table 2 Comparison of Results for the Two Random Variable Case

<i>Method</i>	<i>P_f</i>	<i>% error</i>
Numerical Integration	0.007553	-
Monte Carlo	0.007686	1.8%
Independent	0.010809	43%

Table 3 First- and Second-Order Bounds for the Two Random Variable Case

<i>Bound</i>	<i>Lower</i>	<i>Upper</i>
First-order	0.005793	0.010809
Second-order	0.007689	0.009165

Seven Random Variable Case

The system is identical to the previous example except that all relevant random variables are considered and are described in Table 7.

Monte Carlo simulation was used to compute the baseline solution. 12,000,000 samples were used to obtain a solution with 95% confidence that the error is within 2%. Table 4 lists the solutions using Monte Carlo simulation and the independent event assumption. The solution using the independent event assumption is conservative.

The FORM results for each failure event are listed in Table 8. The MPP information is also included and the correlation between these events is estimated to be $\rho = 0.87$. Therefore, the first and second-order bounds for positively correlated events are computed using Equations 8 and 14 respectively. The bounds are shown in Table 5.

The first-order bounds include the Monte Carlo solution. The probability of system failure is not bounded by the second-order approach. In addition, the upper bound under predicts the probability of system failure. Therefore the second-order bounds approach yields a non-conservative solution.

The error for the second-order bounds is attributed to the linear approximation of the limit-state when using FORM to compute the event probabilities. A more accurate solution of the event probabilities would yield more accurate second order bounds. The intersection probability is correctly bounded according to Equation 13.

Table 4 Case 2: Comparison of Results for the Seven Random Variable Case

<i>Method</i>	<i>P_f</i>	<i>% error</i>
Monte Carlo	0.000842	-
Independent	0.000905	7%

Table 5 Case 2: First- and Second-Order Bounds for the Seven Random Variable Case

<i>Bound</i>	<i>Lower</i>	<i>Upper</i>
First-order	0.000467	0.000905
Second-order	0.00736	0.00819

Conclusions

This paper outlined first- and second- order bounding methods for computing system reliability. A common approach to system reliability is to assume that the events are independent. This approach can lead to large errors in probability of system failure but is conservative for series systems.

While there is some contradiction in the literature, a complete treatment of first-order bounds was presented. Tighter first-order bounds can be obtained if information about how the events are correlated is available. If only event probabilities are available (with no correlation information), then the best that can be done is to compute bounds that cover the range from positive to negative correlation.

Second-order bounds require information about the intersection of the events. In practice the second-order bounds typically use a first-order approximation to the limit-state for each event and the intersection of the two events is estimated by the correlation between the events. For nonlinear limit-states, the second-order

bounds may not actually include the true solution based on the error of the event probabilities of failure or the predicted intersection of the events.

The acceptable error in a solution is subject to the required use of the results. Because of underlying assumptions in the physics of the system performance and uncertain random variable distribution information, predicting the probability of system failure within an order of magnitude may be acceptable.

Acknowledgements

This work was part of the lead author’s master’s thesis in Mechanical Engineering at the University of Texas at San Antonio. The support of Dr. Ronald L. Bagley and Dr. Nestor E. Sanchez of UTSA and Southwest Research Institute is gratefully acknowledged in accomplishing this work.

References

1. Cornell, C. A., 1967, “Bounds on the Reliability of Structural Systems,” *J. of the Structural Div., ASCE*, Vol. 93, pp. 171-200.
2. Kounias, E. G., 1968, “Bounds for the Probability of a Union with Applications,” *Annals of Math. Stat.*, Vol. 39, No. 6, pp. 2154-2158.
3. Ditlevsen, O., 1979, “Narrow Reliability Bounds for Structural Systems,” *J. of Structural Mechanics*, Vol. 7, pp. 453-472.
4. Madsen, H. O., Krenk, S., and Lind, N. C., 1986, Methods of Structural Safety, Prentice-Hall, Inc., New Jersey.
5. Cruse, T. A. editor, 1997, Reliability-Based Mechanical Design, Marcel Dekker, Inc., New York, NY.
6. Cruse, T. A., Mahadevan, S., Huang, Q., and Mehta, S., 1994, “Mechanical System Reliability and Risk Assessment,” *AIAA J.*, Vol. 32, pp. 2249-2259.
7. Ang, A. H.-S. and Tang, W. H., 1984, Probabilistic Concepts in Engineering Planning and Design, Volume II: Decision, Risk, and Reliability, New York: John Wiley & Sons, Inc.
8. Ditlevsen, O. and Madsen, H. O., 1996, Structural Reliability Methods, John Wiley & Sons Ltd., West Sussex, England.
9. Rao, S., 1992, Reliability-Based Design, McGraw-Hill, Inc., New York, NY.
10. Thoft-Christensen, P. and Murotsu, Y., 1986, “Application of Structural Systems Reliability Theory,” Springer-Verlag Berlin, Heidelberg.
11. Wu, Y. -T., Wirsching, P. H., “A New Algorithm for Structural Reliability Estimation,” *J. Engineering Mechanics*, vol. 113, 1987, pp. 1319-1336.
12. Hunter, D., 1976, “An Upper Bound for the Probability of a Union,” *J. of Applied Probability*, Vol. 3, No. 3, pp. 597-603.
13. Xiao, Q. and Mahadevan, S., 1994, “Second-order Upper Bounds on Probability of Intersection of Failure Events,” *ASCE J. Eng. Mech.*, Vol. 120, pp. 670-674.
14. Southwest Research Institute and Rocketdyne, 1995, “Probabilistic Structural Analysis Methods (PSAM) for Select Space Propulsion System Components,” *Final Report NASA Contract NAS3-24389*, NASA Lewis Research Center, Cleveland, Ohio.
15. Riha, D. S., Thacker, B. H., Millwater, H. R., Wu, Y.-T. and Enright, M. P., 2000, “Probabilistic Engineering Analysis Using the NESSUS Software,” Proc. *AIAA/ASME/ASCE/AHS/ASC 41st Structures, Structural Dynamics, and Materials (SDM) Conf.*, Atlanta, Georgia, 3-6 April.

Table 6 FORM Solution for the Two Random Variable Case

RV	g ₁			g ₂		
	X MPP	u MPP	Alpha	X MPP	u MPP	Alpha
Load	32.7350	0.9117	0.35436	35.3553	1.7851	0.70711

Length	12.4057	2.4057	0.93511	11.7851	1.7851	0.70711
--------	---------	--------	---------	---------	--------	---------

Table 7 Case 2: Random Variables for the Seven Random Variable Case

Random Variable	Description	Mean	Standard Deviation	Distribution
P	Point Load	30.0 (lb.)	3.0 (lb.)	NORMAL
L	Beam Length	10.0 (in.)	1.0 (in.)	NORMAL
E	Elastic Modulus	10,000,000.0 (psi)	1,000,000.0 (psi)	NORMAL
B	Beam Base	1.0 (in.)	0.1000 (in.)	NORMAL
H	Beam Height	1.0 (in.)	0.1000 (in.)	NORMAL
δ_0	Displacement Limit	0.06 (in.)	0.006 (in.)	NORMAL
σ_y	Yield Strength	5000.0 (psi)	500.0 (psi)	NORMAL

Table 8 Case 2: FORM Solution for the Seven Random Variable Case

RV	g_1			g_2		
	X MPP	u MPP	Alpha	X MPP	u MPP	Alpha
	$\beta=3.3098$ $p_f=0.000467$			$\beta=3.3274$ $p_f=0.000438$		
LOAD	31.7945	0.5982	0.18072	32.6861	0.8954	0.26910
LENGTH	11.6346	1.6346	0.49389	10.8954	0.8954	0.26910
EMOD	9.3197E+06	-0.6803	-0.20553	1.0000E+07	0.0000	0.00000
BASE	0.9320	-0.6803	-0.20553	0.8904	-1.0959	-0.32935
HEIGHT	0.7443	-2.5567	-0.77247	0.7342	-2.6583	-0.79892
DLIMIT	5.5919E-02	-0.6801	-0.20550	6.0000E-02	0.0000	0.00000
YIELD	5000.0000	0.0000	0.00000	4452.1590	-1.0957	-0.32930